Journal of Chemical Technology and Metallurgy, 49, 6, 2014, 545-550

LAUE FUNCTIONS MODEL VS SCHERRER EQUATION IN DETERMINATION OF GRAPHENE LAYERS NUMBER ON THE GROUND OF XRD DATA

Beti Andonovic, Misela Temkov, Abdulakim Ademi, Aleksandar Petrovski,

Anita Grozdanov, Perica Paunović, Aleksandar Dimitrov

Faculty of Technology and Metallurgy,
SS Cyril and Methodius University, Skopje, Macedonia
E-mail: beti@tmf.ukim.edu.mk

Received 10 June 2014
Accepted 05 October 2014

ABSTRACT

The present study reports data referring to the determination of the layers of graphene samples obtained by electrolysis in aqueous electrolytes and molten salts using a reverse change of the potential applied. The analysis, based on the calculation of 002 XRD peak intensities, is carried out with the application of the Scherrer equation and the Laue functions model. The latter results differ from those obtained on the ground of Scherrer equation but coincide with data obtained by Raman spectroscopy and other methods. This is attributed to the multi-layer structure of the graphene samples studied.

Keywords: graphene, electrochemical production, XRD analysis, layers, Scherrer equation.

INTRODUCTION

Graphene is the building unit of all carbon allotropes [1]. Mechanical exfoliation of graphite, chemical vapor deposition (CVD) on copper film surfaces [2], nanotubes cutting [3], and different electrochemical methods are used for the production of graphene [4, 5]. It can be obtained as monolayer- bi-layer- and multilayer-flakes or sheets [6] depending on the procedure used. The structural characterization of graphene is of outmost importance because its highly unusual properties are largely determined by its structure.

The number of layers in graphene samples can be estimated using XRD data. The latter can be described by the Scherrer equation which is found adequate [7]. But the application of the Laue functions model presents also definite interest as the results it gives are based on the treatment of the graphene thickness distribution. The present study is aimed at the comparative examination of the data obtained with the application of the Scherrer equation the Laue functions model using grapheme samples produced electrochemically in aqueous and non-aqueous electrolytes.

Laue functions model in uniform and non-uniform graphene thickness distribution

The XRD pattern is analyzed using the following Laue functions model which includes graphene thickness distribution and certain parameters [8]:

$$|F|^2 \propto |f(\theta)|^2 \left| \sum_{j=0}^{N} \beta_j e^{jka_j i} \right|^2 \quad (1)$$

where F is a structure factor, N is the number of graphene layer, $|f(\theta)|$ is an atomic scattering factor which varies from 6.00 to 6.15 e/atom with incident radiation ranging from 2 to 433 KeV, $\mathrm{ka_j} = (4\pi \mathrm{d_j} \sin\theta)/\lambda$, where d_j is a lattice spacing between *jth* and *(j-1)th* layer, θ is an angle between the incident ray and the scattering planes, λ is a wavelength of X-ray, and β_j is an occupancy of *jth* graphene layer. The value of β_j is between 0 and 1. The employed equation parameters β_j make it possible to calculate the n-layer graphene regions coverage of the graphene samples produced by the two electrochemical procedures.

Hence XRD intensities of the curves in Fig. 1 (a-d) were calculated thereof.

In Fig. 1 (a-d), theoretical XRD curves are shown,

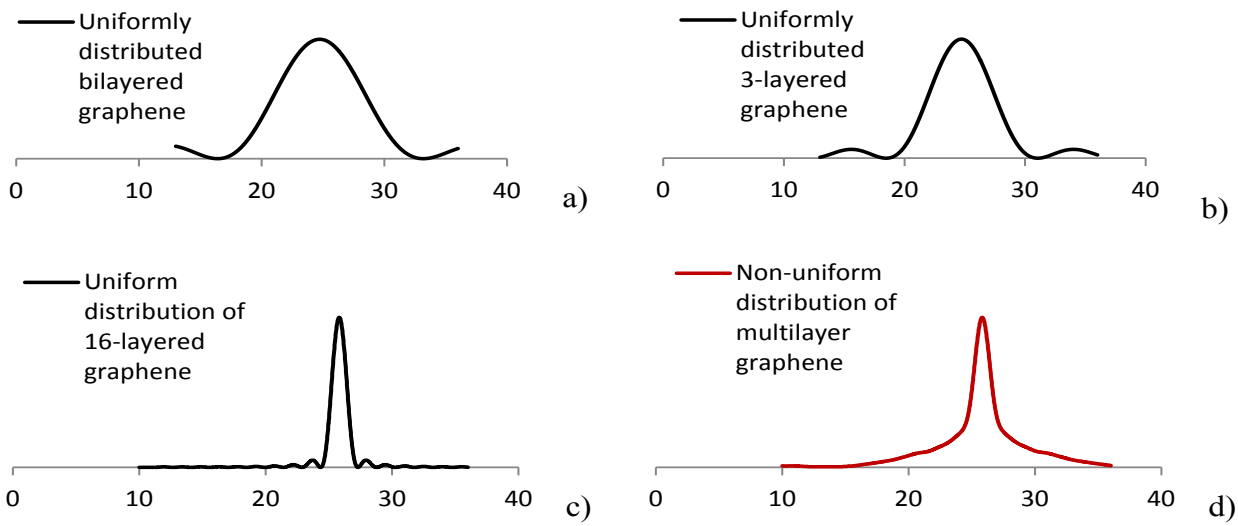

Fig. 1. Theoretical curves obtained by model (1) calculations: a) Theoretical XRD representation of uniformly distributed bilayered graphene; b) Theoretical XRD representation of uniformly distributed 3-layered graphene; c) Theoretical XRD representation of uniformly distributed 16-layered graphene; d) Theoretical XRD representation of non-uniformly distributed multilayered graphene.

with intensities calculated using model (1). The values of employed parameters β_j provide an insight into occupancies of each of the graphene layers and therefore corresponding coverages. In Fig. 1 (a-c) are shown graphenes with uniform thickness distribution, meaning all β_j parameters are equal and therefore highest layer covering 100 % of the area. Thus the curves represent bilayered graphene with 100 % coverage of the second layer, 3-layered graphene with 100 % coverage of the third layer, and 16 layered graphene with 100 % coverage of the 16-th layer.

In Fig.1d is shown a theoretical XRD curve of multilayered graphene with non-uniform thickness distribution. The employed β_j parameters enable the calculation of each of the *jth* layer region occupancy and hence the *jth* layer d_j coverage percentage, where $d_{i-1} = \beta_{i-1} - \beta_i$, i = 2, 3,…, n. The calculations of the coverages are given in Table 1.

From the results given in Table 1, it is clear that the layers are non-uniformly distributed, where the monolayer graphene part covers 60 % of the structure. The average number of graphene layers is calculated as NGL = 3.312.

Scherrer equation and graphene layers number in uniform and non-uniform graphene thickness distribution

The mean dimension of the crystallite perpendicular to the plane of graphene samples L_{002} can be determined by the familiar Scherrer equation:

$$L_{002} = \frac{k \cdot \lambda}{\beta \cos\theta} \quad (2)$$

where k = 0.94 is the shape factor, β is the full width at half maximum given in radians, λ is a wavelength of X-ray, and θ is the angle between the incident ray and the scattering planes. The number of graphene layers N may be determined from the equation $L_{002} = (N-1)d_{002}$, where d_{002} is the average distance between graphene planes [7].

In Table 2 are given the values for the curves, shown in Fig. 1 (a-d).

In the last two columns in Table 2, one may easily compare the values which are calculated results for number of graphene layers. In the case of uniform distribution of the graphene layers, the results are in good agreement, whereas in the case of non-uniform thickness distribution, the values greatly differ. Studies and

Table 1. Occupancies and coverages of each of the layers in grapheme, shown in Fig.1d.

Parameter β_j: j=1,2,…,23	Value	Occupancy of the j-th layer in %	Layer	Share of the j-th layer in %
β_1	1	100	d_1	60
β_2	0.4	40	d_2	10
β_3	0.3	30	d_3	3
β_4	0.27	27	d_4	5
β_5	0.22	22	d_5	2
β_6	0.2	20	d_6	5
β_7	0.15	15	d_7	1
β_8	0.14	14	d_8	1
β_9	0.13	13	d_9	2
β_{10}	0.11	11	d_{10}	2
β_{11}	0.09	9	d_{11}	2
β_{12}	0.07	7	d_{12}	1
β_{13}	0.06	6	d_{13}	1
β_{14}	0.05	5	d_{14}	1
β_{15}	0.04	4	d_{15}	1
β_{16}	0.03	3	d_{16}	1
β_{17}	0.02	2	d_{17}	1
β_{18}	0.01	1	d_{18}	0
β_{19}	0.01	1	d_{19}	0.5
β_{20}	0.005	0.5	d_{20}	0
β_{21}	0.005	0.5	d_{21}	0.4
β_{22}	0.001	0.1	d_{22}	0
β_{23}	0.001	0.1	d_{23}	0.1

analysis that were performed upon graphene samples obtained by two different electrochemical methods, and which are further presented, show that in the case of non-uniform distribution, model 1 is more reliable method for determining the number of graphene layers.

Determining graphene layers number for produced graphene samples with non-uniform graphene thickness distribution

Two graphene samples are analyzed, with the focus on the determination of the graphene layers number. Scherrer equation method and model 1 are compared for obtaining results for the layers number of the graphene samples studied. The graphene samples were prepared by two different electrochemical methods: high temperature electrolysis in molten salt (graphene sample GMSE2) and electrolysis in aqueous solution (graphene sample GAE1), both using non-stationary current regime.

In Fig. 2a, are shown the theoretical curves calculated using model 1, in the case of graphene sample

Table 2. Calculated values for curves shown in Fig. 1a-d from Eq. 2 and model 1.

	θ	FWHM (in Deg)	L_{002} (in nm)	N (by L_{002})	N (by model 1)
Fig.1a	12.36	11	7.17	2.9	2
Fig.1b	12.36	8	9.86	3.7	3
Fig.1c	12.36	1.5	51.6	15.3	16
Fig.1d	12.36	1.5	51.6	15.3	3.3

GMSE2 produced by electrolysis in molten salt at non-stationary current regime. The theoretical curves (1 and 2) are given for comparison to the theoretical curve (3) that exhibits good fitting to the experimental curve. The experimental curve GMSE2 is presented as (4).

In Fig 2b part of the Raman spectrum of sample GMSE2 is given, showing its C-peak. Its position $\mathrm{Pos}(C)_N$ is directly connected to the graphene layers number N, and it varies with N as in the formula [9]:

$$\mathrm{Pos}(C)_N = \sqrt{\frac{2\alpha}{\mu}}\sqrt{1+\cos\left(\frac{\pi}{N}\right)}$$

where $\alpha = 12.8\times10^{18}\ \mathrm{Nm}^{-3}$ is the interlayer coupling, and $\mu = 7.6\times10^{-27}\ \mathrm{kg\,\mathring{A}}^{-2}$ is the graphene mass per unit area.

According to the analysis of the XRD 002 peak and the employed β_j parameters, the j layer region coverages are given in Table 3.

The average value for number of graphene layers for graphene sample GMSE2 is calculated as NGL = 2.4 for the dominant structure (above 75 %) and NGL = 7.43 for the overall structure, by calculations from model 1. Using the Scherrer equation for the number of graphene layers determination, was obtained N = 27.7.

According to the C-peak position, which is the only value from Raman spectra that directly points the number of graphene layers [9], for sample GMSE2 was calculated N = 2.54.

Model 1 stands out as the method giving results in accordance to C-peak calculations for graphene layers number.

In Fig. 3 are shown curves, calculated from the model 1, for graphene sample GAE1 produced by electrolysis in aqueous solution at non-stationary current regime, for $\beta_j \neq 1$, which suggests that the number of graphene layers has a distribution.

The dotted line (1) in Fig. 3 is calculated curve for uniformly distributed monolayer graphene, the line (2) which is narrower than the monolayer graphene line, but broader than the green experimental curve (3) GAE1, is calculated curve for a non uniform distribution of graphene layers number for a 3-layered graphene. The line (4) is calculated curve for a non uniform distribution of graphene layers number for a multi-layered graphene. There is a noticeable discrepancy with the experimental curve due to its asymmetry. However, as the correlation coefficient is $\rho = 0.92$, it provides an insight with a fair accuracy into j-layer graphene regions share. According to β_j parameters, the coverages of n-layer graphene regions are calculated (Table 4).

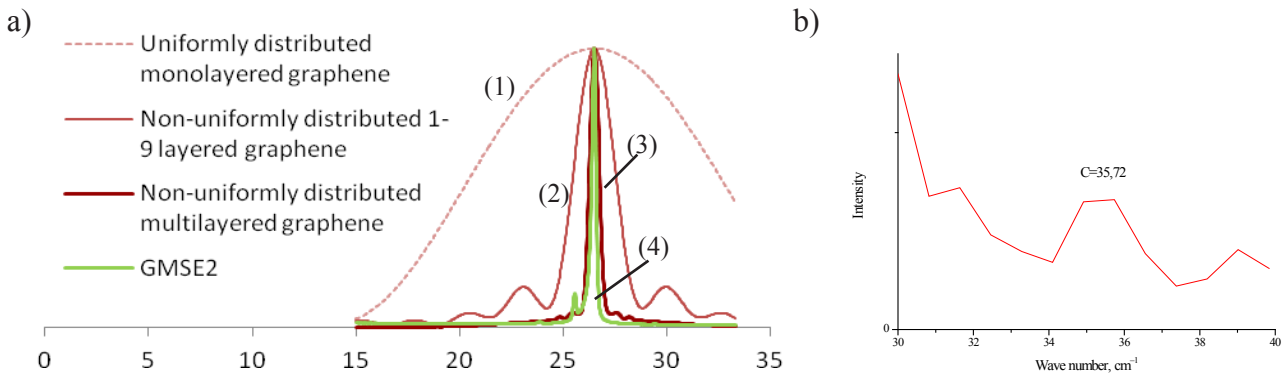

Fig. 2. a) Non uniform multilayer distribution for Sample GMSE2 calculated from model 1;
b) C-peak position in Raman spectrum for graphene sample GMSE2.

Table 3. Coverages of *j*-layer GMSE2 graphene regions.

Monolayer region coverage	~ 18.75%
2 layers region coverage	~ 21.25%
3 layers region coverage	~ 3.75%
4-6 layers region coverage	~ 2.5%
7-8 layers region coverage	~ 2.5%
9-10 layers region coverage	~ 1.25%
> 10 layers region coverage	< 25%

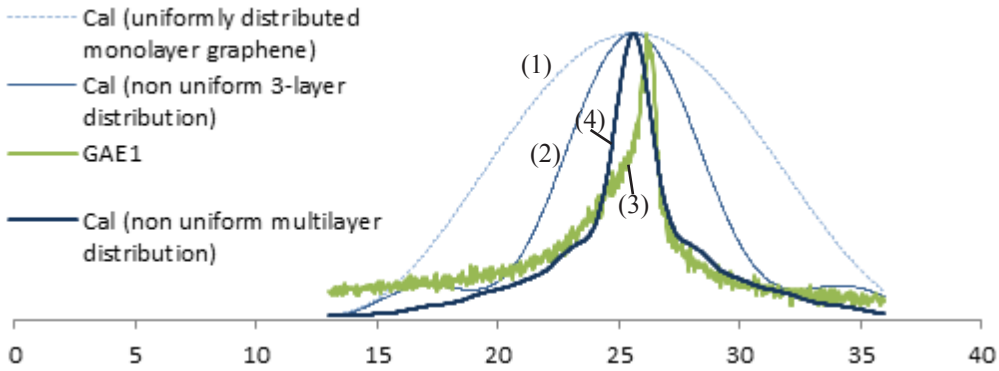

Fig. 3. Non uniform multilayer distribution curve for Sample GAE1 calculated from model 1.

According to these calculations, the dominant structure (above 90 %) is few-layered, and the average value for number of sample GAE1 graphene layers is calculated as NGL = 2.57 for the dominant graphene structure and NGL=4.25 for the overall graphene structure. According to Scherrer equation the number of graphene layers is N = 15.3.

However, considering GAE1 TEM images and GAE1 Raman spectrum analysis results (Fig. 4 a, b), model 1 again stands out as a method producing results which are in accordance with TEM images results and Raman spectrum I2D/IG FWHM ratio. TEM images in Fig. 4 a, clearly indicate high share of few-layer region, particularly monolayer region, whereas from GAE1 Raman spectroscopy in Fig. 4 b, I2D/IG = 1.49, which estimates the number of GAE1 graphene layers as N~4. The obtained number N of graphene layers is in accordance with the number obtained by model 1.

CONCLUSIONS

This study shows that the accuracy of Scherrer equation method for determining the number of graphene layers by XRD data decreases as the level of non-uniformity of graphene thickness distribution increases. Therefore, another method is involved for determining the average number of graphene layers by XRD data in the studied graphene samples. It is a Laue functions model

Table 4. Coverages of *j*-layer graphene sample GAE1 regions.

Monolayer region coverage	~ 40%
2 layers region coverage	~ 10%
3-6 layers region coverage	~ 15%
7-10 layers region coverage	~ 5%
> 10 layers region coverage	< 10%

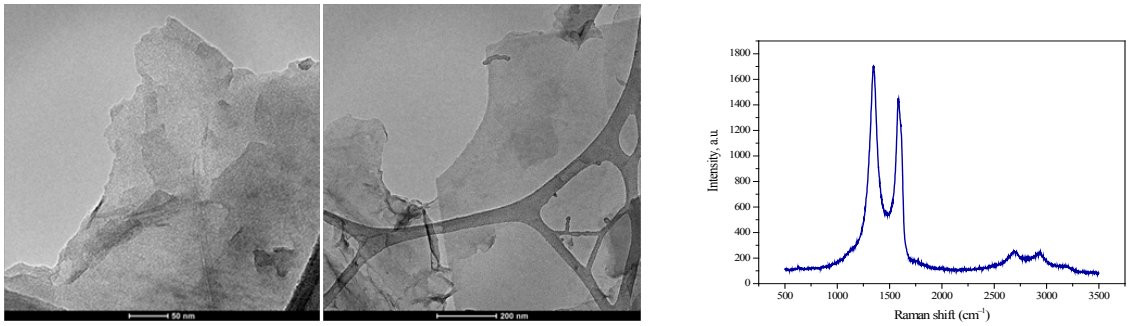

a) b)

Fig. 4. a) TEM images of Sample GAE1 graphene sheets; b) GAE1 Raman spectrum.

which includes graphene thickness distribution and the employed parameters allow calculations of graphene *j*-layer region coverage, thus enabling determination of the graphene layers number.

Graphene samples which are subject of our study are produced by two different methods: high temperature electrolysis in molten salt and electrolysis in aqueous solution, both using non-stationary current regime.

The analysis and comparison of the two methods show that both are in agreement as far as graphene samples that are considered have uniform thickness distribution. However, in non-uniform distribution cases, Laue functions model (model 1) stands out as reliable and in accordance with other methods results. It additionally provides information on graphene samples *j*-layer occupancies and therefore coverages with a fair accuracy. The results relevant to graphene samples produced by electrolysis in aqueous electrolyte and by electrolysis in molten salts, both using reverse change of the applied potential, have shown that these graphene samples are few-layered.

REFERENCES

1. K. S. Novoselov, et al., Two-dimensional atomic crystals, Proc. Natl Acad. Sci. USA 102, 2005, 10451-10453.
2. A. Ismach, C. Druzgalski, S. Penwell, A. Schwartzberg, M. Zheng, A. Javey, J. Bokor, Y. Zhang, Direct chemical vapor deposition of graphene on dielectric surfaces, Nano Letters, 10, 2010, 1542.
3. L. Jiao, L. Zhang, X. Wang, G. Diankov, H. Dai, Narrow graphene nanoribbons from carbon nanotubes, Nature, 458, 2009, 877.
4. A.T. Dimitrov, A. Tomova, A. Grozdanov, O. Popovski, P. Paunović, Electrochemical production, characterization, and application of MWCNTs, DOI 10.1007/s10008-012-1896-z, J Solid State Electrochem., 17, 2013, 399-407.
5. C. Schwandt, A.T. Dimitrov, D J. Fray, High-yield synthesis of multi-walled carbon nanotubes from graphite by molten salt electrolysis, Carbon, 50, 2012, 1311-1315.
6. C.T.J. Low, F.C. Walsh, M.H. Chakrabarti, M.A. Hashim, M.A. Hussain, Electrochemical approaches to the production of graphene flakes and their potential applications, Carbon, 54, 2013, 1-21.
7. B.K. Saikia, R.K. Boruah, P.K. Gogoi, A X-ray diffraction analysis on graphene layers of Assam coal, J. Chem. Sci., 121, 1, 2009, 103-106.
8. A. Ruammaitree, H. Nakahara, K. Akimoto, K. Soda, Y. Saito, Determination of non-uniform graphene thickness on SiC (0 0 0 1) by X-ray diffraction, Applied Surface Science, 282, 2013, 297- 301.
9. Andrea C. Ferrari, Denis M. Basko, Raman spectroscopy as a versatile tool for studying the properties of graphene, Nature Nanotechnology, 8, 2013, 235.